LAWRENCE
LIVERMORE
NATIONAL
LABORATORY

LLNL-JRNL-484106

Seismic Velocity Structure at the Southeastern Margin of the Arabian Peninsula

S. Al-Hashmi, R. Gok, K. Al-Toubi, Y. Al-Shijbi, I. El-Hussain, A. J. Rodgers

May 17, 2011

Geophysical Journal International

Disclaimer

Seismic Velocity Structure at the Southeastern Margin of the Arabian Peninsula

Al-Hashmi S. [1], Gök R. [2] , Al-Toubi K. [1], Al-Shijbi Y. [1], El-Hussain I. [1] and Rodgers A.J. [2]

[1] Earthquake Monitoring Center, Sultan Qaboos University, Muscat, OMAN

[2] Lawrence Livermore National Laboratory, Livermore, CA, USA

Abstract

The lithospheric structure in Oman has been determined by analyzing teleseismic P-receiver functions recorded at broadband and short-period seismic stations of the Oman Seismological Network. Lithospheric structure is obtained by jointly inverting receiver functions and Rayleigh wave group velocities derived from continental-scale surface wave tomography of Pasyanos (2005). We observe relatively thick crust (40-48 km) within the ophiolite formed mountains in northern Oman. The crustal thickness is about 35 km within the passive continental margin of the southern Oman region. Uppermost (< 5 km) crustal shear wave velocities are faster in the northern ophiolite regions compared to the southern Oman region, while shear velocities in the middle crust are faster in the Southern Oman region compared to the ophiolite region. This observation coincides well with cretaceous to Eocene marine platform sequences overlying Precambrian to Cambrian basement of the southern part. Joint inversion analysis shows that the Moho depth of Oman varies from 34 km in the southern region to 48 km in the northern part.

Introduction

Oman is located in the southeastern part of the Arabian Peninsula surrounded by the divergent, transform and convergent plate boundaries. The Arabian plate moves to the north direction away from African plate at a rate of 18 +/-2 mm/yr relative to the stable Eurasian plate (McClusky et al., 2000; Relinger et al., 2006). The continental crust of the Arabian plate collides with the Eurasian plate along the Bitlis and Zagros suture zone in the north and northeast part of the Arabian plate. Zagros accommodates part of the convergence between Arabia and Eurasia and it continues along the Makran subduction zone. The northern Oman Mountains form an arc extending for 700 km from Musandam in the north to the east coast at Ras Al-Hadd. These mountains define an obduction zone where the mid-oceanic rocks and deep ocean sediments of the ancient Tethys Ocean were thrust upwards and over the continental shelf and slope rocks of the Arabian platform (Glennie et al. 1973; Glennie et al. 1974; Glennie 1992).

Oman is surrounded by subduction type plate margin (Makran), Oman Sea in the north , by divergent type plate boundary in the Gulf of Aden in the south and by the transform type margin of the Owen-Murray Fracture zone in the east. The Owen-Murray Fracture zone separates the Arabian and Indian plates, along a line just about parallel to the east Oman coastline.

The tectonics of the Northern Oman Mountains can be divided into three main units underlain by pre-permian basement that consists of siltstone and sandstone. The first unit is the Permian to Cretaceous autochthonous rocks called Hajar Supergroup. It can be subdivided into several groups that make up a thick sequence of mainly shallow marine shelf carbonates ranging in age from middle Permian to mid-Cretacous overlain by late cretaceous formation called Muti. It consists of shales and marls containing irregular lenses or thicker sequences of limestone conglomerate, coarse lithoclastic limestone turbidites and some radiolarian chert with the total thickness of about 2.2 km. The Permian to Cenomanian limestone sequence of the Hajar Supergroup is considered to be the result of mainly shallow marine sedimentation over the continental margin of south east Arabia (Glennie et al., 1973).

The second unit is the Late Triassic to Mid Cretaceous called Hawasina. It forms a structural complex subdivided into several tectonically bounded lithostratigraphic units. It consists mainly of conglomeratic limestone, lithoclastic grainstone turbidites and quartz-sand turbidites with some radiolarian cherts (Glennie et al. 1973; Lippard et. Al. 1982; Robertson et al. 1990; Hugh 2000) . The total thickness of Hawasina is about 3.2 km. This structural and stratigraphic complex tectonically overlies the Hajar Supergroup and overlain by the ophiolites of the Semail nappe which forms the third unit (Glennie et al. 1973).

The Semail ophiolite in the Oman Mountains is the world's largest and best preserved thrust sheet of oceanic crust and upper mantle (Searle et al. 1999). It was emplaced into the Arabian continental margin during the Late Cretaceous closure of the Tethys ocean (Gnose, E. 1996). The ophiolites originated 96-94 Ma at a spreading center above a northeast-dipping subduction zone and form basic or ultrabasic rocks. Oman Mountains have been considered to be an example of a 'foreland type' fold-and-thrust belt (Elliott, 1976). The Semail ophiolite nappe is broken by cross-strike faults into several blocks (Nicolas et al., 1988). The present day Semail ophiolites are around 10-12 km thick (Glennie et al., 1974; Hopson et al., 1981; Shelton, 1990). Present day morphology of the Oman mountains is due to Tertiary, post-early Miocene (Le Métour et al., 1995) over-thrusting and folding. In Northern Oman Mountains, both Hawasina and the Semail ophiolite are overlain unconformably by late Maastrichtian shallow marine limestones (Glennie et al. 1973; Glennie et al. 1974).

The Dhofar region (southern part of Oman) is about 250 km from an active spreading ridge to the south in the Gulf of Aden. This southern margin near the divergent plate boundary of Oman comprises a similar structure to the Arabian platform where the basement is overlaid by the marine platform sequences. Tectonically, the southern part of Oman starts with a crystalline and metamorphic basement of Late Proterozoic age overlain by upper Cretaceous strata represented by Sarfait Formation which is a massive, micritic limestone with rudist biostromes. It has a thickness of about 120m. The later is overlain uncomfortably by the Hadhramaut Group - Paleocene (Thanetian) to late Eocene (Priabonian) in age - which consists of three, shallow-marine, carbonate shelf units that have a thickness of about 1100 m. The Dhofar Group (Late Eocene – Miocene) lies uncomfortably on the upper part of the Hadhramaut Group. It has a thickness of more than 1200m where more than 700m is calcareous turbidities of the Mughsayl formation. The top section is a shallow-marine conglomeratic limestone (Adawnib formation; middle Miocene) of thickness varying from about 40 to 70 m. (Roger et al., 1989 ; Platel, J. P., and Roger, J., 1989)

Previous studies of the crustal and uppermost mantle structure in Oman were mostly based on Bouger gravity data (Shelton, 1990). Ravaut et al. (1997) jointly interpret Bouguer anomaly and seismic profiles interms of crustal structure. They merged gravity and seismic data over the Zagros-Makran-Oman to constrain the geometry of sediment deposits and ophiolite nappes. Then, they developed 2D elastic models to explain observed deflection of the Arabian Lithosphere due to loading effects (ophiolites, topography and sedimentary loads). They show that the gravity anomaly in northern Oman is characterized by a high amplitude negative-positive couple. They found that the large scale gravity low, extended from the Zagros to northeast Oman can be interpreted as evidence of the elastic deflection of the Arabian Lithosphere and its Moho. Al-Lazki et al., (2002) studied a southwesterly oriented crustal transect of the Oman Mountains. They combined seismic reflection profiles, well-data, gravity and teleseismic receiver functions and found that the Moho at the coastal range is slightly shallower than the southwest part of Jebel Akhdar Mountains. The basement was found to be 9 km near the mountain region. They also found a variable thickness of ophiolites from 1 to 4 km. Tiberi et al. (2007) analyzed receiver functions of broadband array in southern Oman (Dhofar). They found the average crustal thickness is about 35 km beneath the northern rift flank of the Gulf of Aden, in Dhofar region.

In this paper, we combined the regional/global Rayleigh wave dispersion models with receiver functions that were recorded by the seismic network of Oman. Receiver functions primarily contain information on velocity contrasts, while surface waves are sensitive to the average shear velocity with depth. By performing a joint inversion we reduce the limitations of each method, resulting in a more robust shear wave models (Gök et al., 2001; Julia et al., 2000, 2003).

Oman Seismic Network

The seismic network consists of thirteen remote stations transmitting data in real time via satellite to the central data acquisition system in the Earthquake Monitoring Center located at Sultan Qaboos University (SQU). Ten of the remote stations are short period and the other three are broadband. Each short period station is equipped with three short period SS-1 seismometers, a Quanterra (Q730BL) data-logger, a satellite system and a solar power system. Broadband stations (ASH, BAN and SHA) consist of STS-2 type seismometers, a Quanterra (Q330) datalogger, a satellite system and a solar power system**.** The Q330

datalogger records 6 broadband high resolution channels at 100 sps. Stations of Omani network are concentrated at the northeastern and southern parts of the Sultanate of Oman.

Methodology

In this study, shear wave velocity structure in Oman is obtained from jointly inverted teleseismic receiver functions and surface waves. Teleseismic P-wave receiver functions are widely used to constrain crustal and upper-mantle velocity and discontinuity structure beneath a seismic station by isolating the *P–S* converted waves from the coda of the *P* wave (Langston, 1979; Ammon et al. 1991). Teleseismic events (Mb>= 5.5) ranged in distance between 44 to 90 degrees and they spanned early 2005 to 2007. A time domain iterative deconvolution technique (Liggoria and Ammon, 1992) was used with a Gaussian width factor of a=1.5 and a=2.5. We determined both the radial and tangential receiver functions. Guassian width factors with values of 1.5 and 2.5 correspond to pulse widths of approximately 1.4 and 1.05 seconds. We obtained about 50 teleseismic receiver function candidates at each station. As expected, receiver functions at short period stations were noisier than those at the broadband stations due to its short-period response. We strictly eliminated the noisier receiver functions by visual inspecting each data set, according to the clearness and coherence of the recognized multiple phases for stacking (Figure 2) which brought them down to about 20 receiver functions at short period stations. Figure 2 shows the selected individual radial and transverse component receiver functions for both Gaussian width factors. In most cases, the receiver functions show a clear Ps_{MOHO} conversion at 4-6 seconds after the main P-wave pulse at 0 seconds. In some cases, however, the Ps amplitudes were quite emergent (e.g. SMD, JMD, BSY, BAN), while other stations had very clear Ps_{MOHO} arrivals (e.g. RBK, SHA, ASH, HOQ, BID). Some of the receiver functions show large amplitude phases possibly related to intracrustal conversions. This is probably due to ophiolites or sediments causes conversion at those boundaries (Figure 2). HOQ, BID and ABT station receiver functions had a negative pulse near the P arrival which could be related to a higher velocity ophiolite emplacement on relatively lower velocity of the upper crust. Another could be a biased azimuthal sampling of a dipping and/or anisotropic layer.

We obtained the Rayleigh wave group velocities from Pasyanos et al., (2005). Pasyanos made dispersion measurements for about 30,000 Rayleigh wave paths and incorporated measurements from several other researchers into a single inversion for Eurasia.

His tomographic inversion used a variable smoothness with the conjugate gradient method which produces higher-resolution models where the data concentration allows. The current results include both Love and Rayleigh wave inversions across the region for periods from 7 to 100 s on a 1° × 1° grid and at resolutions approaching 1° under some conditions. Figure 3 shows the plot of the Rayleigh wave dispersion curves extracted from the Pasyanos (2005). A large difference is observed between the periods of 15 to 50 sec. SHA located in the Dhofar region has the fastest dispersion curve, while ASH in the Oman Mountains is the slowest.

As was pointed above, Rayleigh surface-wave dispersion measurements are sensitive to broad average earth structure while receiver functions are highly sensitive to the velocity contrasts. They are both sensitive to the SV wave velocity structure in the lithosphere. By combining these two complementary data types, we can reduce the non-uniqueness of the individual data sets and narrow the range of models that are compatible with both measurements (Julia et al., 2000). Julia et al. (2000) implemented the receiver function and surface wave joint inversion technique using the joint prediction error. In this technique, the receiver functions and Rayleigh wave dispersion misfits are combined into a single algebraic equation and each data set is weighted by an estimate of the uncertainty in the observations. Julia et al. (2000) formulated a linearized shear velocity inversion that is solved using a damped least-square method.

The system of equations is inverted using the partial derivative matrices for the dispersion and RF estimates. The data are weighted to equalize the contribution of each data set by dividing the individual prediction error by the number of data points and the variance. The smoothness and damping parameter control between the data fit and model smoothness. An influence parameter, p, controls the contribution of each data type to the inversion. We performed inversion using a range of p values of 0.3, 0.5 and 0.7. If p=0 the inversion is only for receiver function and p=1 is only for surface waves.

In order to avoid bias we performed inversions using various starting models. We choose two different starting models from average continental velocities with a similar geologic history. One is a simple two-layered model with shallow Moho depth (25 km) and the second one has thick (6km) sedimentary layer with a deeper Moho (35km). We used a rather thin (2-2.5 km) layer in the upper layers of the model which provides some freedom in the inversion to resolve the fine structure. We increased the layer thickness to 3-4 km for the lower crust and upper mantle. The range of smoothness (0.6 and 0.7) and the influence parameters (0.3, 0.5 and 0.7) are used to test the effect on the final model. During the

inversion, convergence was achieved in five to six iterations. The uniqueness of the inversion results was investigated by performing the inversion with two different starting models along with different influence and smoothness parameters. The inversions with different starting models and parameters resulted in some variation in the deeper velocities (>50 km) for stations SHA, ABT, RBK, WHF and WBK. However, the crustal models are relatively insensitive to different starting model or inversion parameters. We observed this starting model sensitivity at some stations (e.g. ABT, RBK, SHA, JMD, and WBK). ABT, RBK and SHA are all located in Dhofar region. The deeper part of the model (between crust and upper mantle) shows a large range of variation within this southern margin. It could be the result of poor resolution of surface wave dispersion curves.

Results

We show the observed receiver function stack and synthetic along with the observed and predicted Rayleigh wave dispersion curves in Figures 4a and 4b. The synthetics are shown as red and data is the black solid line. The upper left panel shows the receiver functions of two different Gaussian widths (a=2.5 upper and a=1.5 lower trace). The lower left panel is the observed and synthetic surface wave dispersion curves. The starting models are shown as black solid lines on the right panel.

We found a good fit of receiver functions for all iterations of the individual joint inversion while improving the dispersion curve fits. The Moho depth for each station was chosen where the shear velocities showed an increase or where the shear velocity exceeded at least a value of 4.2 km/s. We chose 4.2 as it provided a consistent estimate of the expected Moho boundary when combined with the gradient. This low value might be due to slightly lower Sn velocity (S wave travelling at the Moho interface) which might be caused by the smoothness in inversion and some irregularities of the receiver functions amplitudes. Moho depths in northern and southern part of Oman show great variability with values in northern Oman about 7-8 km deeper than those in southern Oman. The shallowest Moho depth was 34 km in southern Oman, while the thickest crust is observed at station BAN (48km) in northern Oman.

Northern Oman

Station BAN (broad-band) is located in the Musandam Peninsula. The receiver functions of this station show a very weak and late arriving Moho converted phase at 7 sec. It is even harder to observe at higher Gaussian filtered (2.5) receiver functions (Figure 2). The inversion results show a very low gradient down to 56 km. Because of the nature of inversion process and the surface wave sensitivity kernels, if the Moho conversion is not observed as a very prominent arrival in the receiver functions, the resulting model will not show a large gradient. The receiver function amplitudes are not always very stable that they may not reflect the actual sharpness of the Moho. A slight increase of a shear wave velocity is observed at 40 km.

ASH, the second broadband station of northern Oman is located at the mixture of ophiolite outcrop and alluvial deposits. This receiver function shows a very consistent intracrustal discontinuity and it is reflected as a thick (8 km) slow sedimentary layer. We tried forward modeling the receiver functions and surface waves to test the nonuniqueness of the joint inversion. The crustal model with 5km, the Moho conversion is seen clearly on both Gaussian filtered receiver functions at around 45 km. Stations HOQ and BID show similar lithospheric velocity models with a few kilometers of fast (~3.6 km/s) upper crustal discontinuity overlaid on relatively slow (2.6 km/s) layers. Ps conversion is very strong at HOQ than BID with almost the same arrival time (4.9 sec). Both HOQ and BID show small variations at the lower (below 70 km) part of the model. The strong effect of ophiolites is observed at HOQ, BSY and BID (Figure 4a, 5 km depth slice). The expected thickness of the ophiolite is around 4 km (Al-Lazki, 2002). ARQ station shows very consistent output models for any variation on the input parameters. Few kilometers of slow upper crust is overlaid by a smooth gradient of increasing velocity. The Moho converted phase is seen at 4.0 sec. We determined the Moho thickness for this station to be about 40 km. Receiver functions at BSY and SMD are noisy, but show similar sensitivity in the upper crust and their output models are broadly similar. However, the crustal thickness at SMD and BSY appears to be shallowest in the region (38 km). This might be the result of poor quality receiver functions due to the limitations of the short-period instrumentation.

The thickness of the crust in northern Oman as determined by the joint inversion method ranges between 38 km in the southern part of Oman Mountains to 48 km in the northern part. These crustal thicknesses in the region reflect the obduction of the ophiolite over the Arabian plate. There is indication that the average ophiolite thickness can be as thick

as 5 km. The thicker crust in northern Oman determined in this study is consistent with the nature of the region being under a convergent plate boundary in the past, which created the Oman Mountains.

Southern Oman (Dhofar Region)

Station SHA (broad-band) is located in Dhofar region. It shows a nice fit in the crust with various starting models. This station is located on Hadramuth group which is characterized by pre-rifting sediments. RBK, WHF and ABT are the short period stations located in the southern-most Oman in the Dhofar region. Strong upper crust discontinuity at 2-6 km is observed when trying to fit the trough following the P- arrival at ABT. The crust is thinner in this region (34-36 km) at stations SHA, RBK, WHF and ABT as compared to northern Oman. Lower crustal velocities are significantly higher in the Dhofar region compared to northern Oman. Upper crustal layers (2-3 km) are dominated with Tertiary southern Dhofar deposits down to 2-3 km (see SHA, ABT, RBK, WHF at Figures 4a, 4b, 7 and 8).

When compared to some of northern Oman stations (ARQ, HOQ, BID and SMD) we found that they have higher Vs velocities at shallow depths. This could be the effect of high velocity ophiolites. We do not know the exact depth and thicknesses of those ophiolites but we can conclude that we see a certain trend of higher velocities within those stations. A significant difference is also observed at 20 km depth. The lower crustal velocities at northern Oman are 0.3-0.4 km/s lower than that of the southern stations.

Vp/Vs Ratios

After obtaining the average crustal thicknesses through joint inversion we used them as *a priori* information of crustal thickness. We took those crustal thicknesses from the inversion results (Table 1) and within a depth search range of ±3km, we calculated the Vp/Vs ratios for crustal multiples of Ps to find average Vp/Vs ratio in the crust. The average S-velocities (Vs) are already obtained through inversion, however, this will constrain the Poisson's ratio. If clear Moho multiples provided by good *Ppms* and *Psms* multiples of the converted *Pms* phase at the Moho are available, one can search Vp/Vs (k) ratio versus Moho depth (h). We used the grid search approach of Zhu & Kanamori (2000). The method sums the theoretical onsets of multiples within given range of k and h values. The maximum

amplitude at this stacking is the best h and k values for that particular station. The computer code written by Julia and Mejia (2004) is used to estimate the maximum amplitude and to calculate errors with the bootstrap technique of 200 times randomly generated subsets. Receiver functions of short-period stations are noisier and we did not observe clear multiples compared to seismograms from broadband stations, however, we included them in the stacking technique. We used Vp=6.4 km/s as average P velocity of the Arabian Platform model (Pasyanos, 2000) at the northern Oman stations and Vp=6.2 km/s in southern Oman as suggested by Tiberi et al. (2007). We are aware of the effect of incorrect average crustal *P* velocity however we have constrained the Moho thicknesses here. Figure 6 shows the best fitting h-k plots of one example station, ASH is a broad-band station in northern Oman. The maximum amplitude obtained is ~43 km Moho depth at station ASH and ~33 km Moho depth at ABT (a short period station in southern Oman). Vp/Vs ratios corresponding to those values are 1.79 and 1.77 respectively. The Moho depth for those maximum amplitudes is slightly off from our average depth through the inversion (Table 1) at maximum ±2km. This is acceptable within the sensitivity of the receiver function inversion. The average Vp/Vs ratio of nine stations in northern Oman is 1.69. This value is lower than the average in southern Oman (Vp/Vs=1.84).

Conclusion

We performed a joint inversion of receiver functions with Rayleigh wave dispersion curves at the Oman Seismic Network stations. Oman Seismic Network stations are located at two important geological provinces. The first is in northern Oman and characterized with one of the most significant ophiolite outcrops in the world. The second is in the southern part of Oman and is at the continental margin of the young rifting flank of Gulf of Aden, southern Oman. Major differences of lithospheric structure are observed in those two regions.

The variation in thickness ranges from thinner (34 Km) in the south near a divergent plate boundary to thicker (48 Km) in the north near a convergent plate boundary. These estimates of Moho depths are consistent with the past and current tectonic setting and plate boundaries surrounding Oman. Tiberi et al. (2007) found an average Moho thickness to be around 36km (Figure 8) and the Vp/Vs value of ~1.8 in southern Oman, Dhofar region. They concluded that the crust in Dhofar reflects the break-up related transition from Arabian platform to extension zone. Sedimentary cover (pre-rifting, syn-rifting and post-rifting) is

also responsible for higher Vp/Vs ratio. The results of this study for Moho depths in southern Oman are consistent with the Tiberi et al. (2007) results. The southern part of Oman is at the trailing edge of the Gulf of Aden rift system. Rifting generally leads to sagging and thinning of the crust. The relatively thinner crust in the south is consistent with crustal thickness found at divergent plate boundaries.

Ophiolites are characterized by high velocities (up to Vs=3.9 km/s). Since HOQ, BSY and BID stations are located on those ophiolite outcrops, the velocity obtained in this study for those stations in the upper crust is consistent with the higher velocity in the ophiolites. ASH, ARQ and JMD are good examples of how the strong low sedimentary layers are indicated in the upper crust. Prepared in part by LLNL under Contract DE-AC52-07NA27344.

References

Al-Lazki, A. I., Seber, D., Sandvol, E., and Barazangi, M., 2002. A crustal transect across the Oman Mountains on the eastern margin of Arabia, *GeoArabia*, **7**(1), 47-78.

Ammon, C. J., G. E. Randall, and G. Zandt, , 1991. On the Nonuniqueness of Receiver Function Inversions J. Geophys. Res., 95, 15,303– 15,318,.

Ammon, C. J., and G. Zandt, 1993. Receiver structure beneath the southern Mojave block, California, Bull. Seism. Soc. Am., 83, 737– 755,.

Christensen, N. I., 1978. Ophiolites, seismic velocities and oceanic crustal structure, Tectonophysics, 47 , 131-157.

Christensen, N.I., Smewing, J.D. 1981. Geology and seismic structure of the northern section of the Oman ophiolite, *J. Geophys. Res.*, Volume 86, Issue B4, p. 2545-2555.

Dickson A.P.., 1986. Preliminary Assessment of the Earthquake Hazard in the Sultanate of Oman. Consultancy Mission Report Prepared for the Sultanate of Oman and the United Nations Development Program(UNDP).

Elliott, D., 1976, The motion of thrust sheets, *J. Geophys. Res.* **81**: 949–963.

Glennie, K.W., Boeuf, M.G., Hughes-Clarke, M.H.W., Moody-Stuart, M., Pilaar, W.F., and Reinhardt, B.M., 1973. Late Cretaceous Nappes in Oman Mountains and Their Geologic Evolution. The American Association of Petroleum Geologists Bulletin, V. 57,No.1, pp 5-27.

Glennie, K.W., Boeuf, M.G., Hughes-Clarke, M.H.W., Moody-Stuart, M., Pilaar, W.F., and Reinhardt, B.M., 1974. Geology of the Oman mountains. In: Verhandelingen Koninklijk Nederlands Geologisch Mijnbouwkundidg Genootschap Transactions, 31. 423.
Glennie, K.W., 1992. Plate Tectonics & the Oman Mountains, Tribulus, 2(2)., pp 11-21.

Glennie, K.W., 1997. Evolution of the Emirates' Land Surface: an Introduction. Perspectives on the United Arab Emirates**"**, pp. 17-35) , Trident Press, Standbrook House, 2-5 Old Bond Street, London WIX 3TB.

Gnos, E. and Nicolas, A., 1996. Structural evolution of the northern end of the Oman Ophiolite and enclosed granulites. Tectonophysics, V. 254, pp 111-137.

Gök, R., Pasyanos, M. Zor, E., 2007. Lithospheric structure of the continent-continent collision zone: eastern Turkey, *Geophys. J. Int.* , **169** (3), 1079–1088.

Gök R., Mahdi H., Al-Shukri H. and Rodgers A. J., 2007. Crustal structure of Iraq from receiver functions and surface wave dispersion: implications for understanding the deformation history of the Arabian–Eurasian collision. *Geophys. J. Int.* **Volume 172 Issue 3, Pages 1179 – 1187.**

Hopson, C. A., 1981. Geologic Section Through the Semail Ophiolite and Associated Rocks along a Muscat-Ibra Transect, Southeastern Oman Mountains. Journal of Geophysical Research, Vol. 86, No. B4, PP. 2527-2544.

Hugh Wilson, H., 2000. The Age of the Hawasina and Other Problems of Oman mountain Geology. Journal of Petroleum Geology, vol. 23 (3), pp 345-362.

Julià, J., Ammon, C.J., Herrmann, R.B. Correig, A.M., 2000. Joint inversion of receiver functions and surface-wave dispersion observations, *Geophys, J. Int.* , **143** , 99–112

Julià, J., Ammon, C.J. Herrmann, R.B., 2003. Lithospheric structure of the Arabian Shield from the joint inversion of receiver functions and surface-wave group velocities, *Tectonophysics* , **371** , 1–21.

Julia, J., Mejia, J., 2004. Thickness and Vp/Vs ratio variation in the Iberian crust. Geophysical Journal International 156, 59–72.

Langston, C. A. 1979. Structure under Mount Rainier, Washington, inferred from teleseismic body waves. *J. Geophys. Res.* **84,** 4749–4762.

Le Métour, J., Michel, J.C., Béchennec, F., Platel, J.P. and Roger, J., 1995. *Geology and Mineral Wealth of the Sultanate of Oman*, Directorate General of Minerals Publication, Sultanate of Oman, 285 pp.

Liggoria, J.P., and C.J.Ammon, 1999. Iterative deconvolution and receiver function estimation, *Bull. seism. Soc. Am.*, **89**, 1395–1400.

Lippard, S J, Shelton, A W and Gass, I G., 1986 . The Ophiolite of Northern Oman, memoir no 11, published for The Geological Society by Blackwell Scientific Publications, ISBN 0-632-01587-X.

Lippard,S. J., Smewing,J. D., Rothery, D. A. and Browning,P., 1982. The geology of the Dibba zone, northern Oman mountains; a preliminary study. Journal of the Geological Society, London, Vol. 139, pp 59-66.

McClusky S., Balassanian S., Barka A., Demir C., Ergintav S., Georgiev I., Gurkan O., Hamburger M., Hurst K., Kahle H., Kastens K., Kekelidze G.; King R., Kotzev V., Lenk O.,

Mahmoud S., Mishin A., Nadariya M., Ouzounis A.; Paradissis D., Peter, Y., Prilepin M., Reilinger R., Sanli I., Seeger H., Tealeb, A., Toksöz M. N., Veis G., 2000. Global Positioning System constraints on plate kinematics and dynamics in the eastern Mediterranean and Caucasus: Journal of Geophysical Research, v. 105, p. 5695-5719.

Pasyanos, M. E. 2000, Predicting Geophysical Measurements: Testing a Combined Empirical and Modelbased Approach Using Surface Waves, Bull. Seismol. Soc. Am. 90, 790–796

Pasyanos, M.E. 2005. A variable-resolution surface wave dispersion study of Eurasia, North Africa and surrounding regions, J. Geophys. Res., 110, B12301, doi:10.1029/2005JB003749.

Platel, J. P., and Roger, J., 1989. Evolution ge´odynamique du Dhofar (Sultanat d'Oman) pendant le Cre´tace´ et le Tertiaire en relation avec l'ouverture du golfe d'Aden, Bull. Soc. Geol. Fr., 2, 253–263.

Ravaut, P., Bayer, R., Hassani, R., Rousset, D. and Al Yahya'ey, A., 1997. Structure and evolution of the northern Oman margin: gravity and seismic constraints over the Zagros-Makran-Oman collision zone. Tectonophysics V. 279, pp 253-280.

Reilinger, R. *et al.*, (2006). GPS constraints on continental deformation in the Africa-Arabia-Eurasia continental collision one and implications for the dynamics of plate interactions, *J. geophys. Res.,* **111,** doi:10.1029/2005JB004051.

Roger, J., Platel, J. P. , Cavelier, C. and Bourdillon-de-Grisac, C., 1989. Donne´es nouvelles sur la stratigraphie et l'histoire ge´ologique du Dhofar (Sultanat d'Oman), Bull. Soc. Geol. Fr., 2, 265–277.

Robertson, A H F, Searle, M P and Ries, A C., 1990. The Geology and Tectonics of the Oman Region, special publication no 49, The Geological Society, ISBN 0-903317-46-X.

Searle, M. and Cox J. 1999. Tectonic setting, origin and obduction of the Oman ophiolite. Geological society of America Bulletin, Vol. 111, No.1, pp. 104-122.

Shelton, A.W., 1990, The Interpretation of gravity data in Oman: constraints on the ophiolite emplacement mechanism. In A.H.F. Robertson, M.P. Searle and A.C. Ries (eds), *The Geology and Tectonics of the Oman Region*, Geol. Soc. Lond. Spec. Publ. No. 49, pp. 459–471.

Tatar M., Hatzfeld D., Martinod J., Walpersdorf A.[1], Ashtiany M.[2] and Chéry J. 2002. The present- day deformation of the central Zagros from GPS measurements. Geophysical Research Letters, Vol 29.

Tiberi C., Leroy S., d'Acremont E., Bellahsen N., Ebinger C., Al-Lazki A. and Pointu A., 2007. Crustal geometry of the northeastern Gulf of Aden passive margin: localization of the deformation inferred from receiver function analysis. *Geophys. J. Int.*(2007) **168,** 1247–1260.

Zor E., Sandvol E., Gurbuz, Turkelli N., Seber D. and Barazangi M., 2003. The crustal structure of the East Anatolian plateau (Turkey) from receiver functions, Geophysical Research Letters, VOL. 30, NO. 24, 8044, doi: 10.1029/2003GL018192.

Zhu L., 2000. Moho Depth Variation in Southern California from Teleseismic Receiver Functions. J. Geophys. Res.,, VOL. 105, NO. B2, PAGES 2969–2980, FEBRUARY 10.

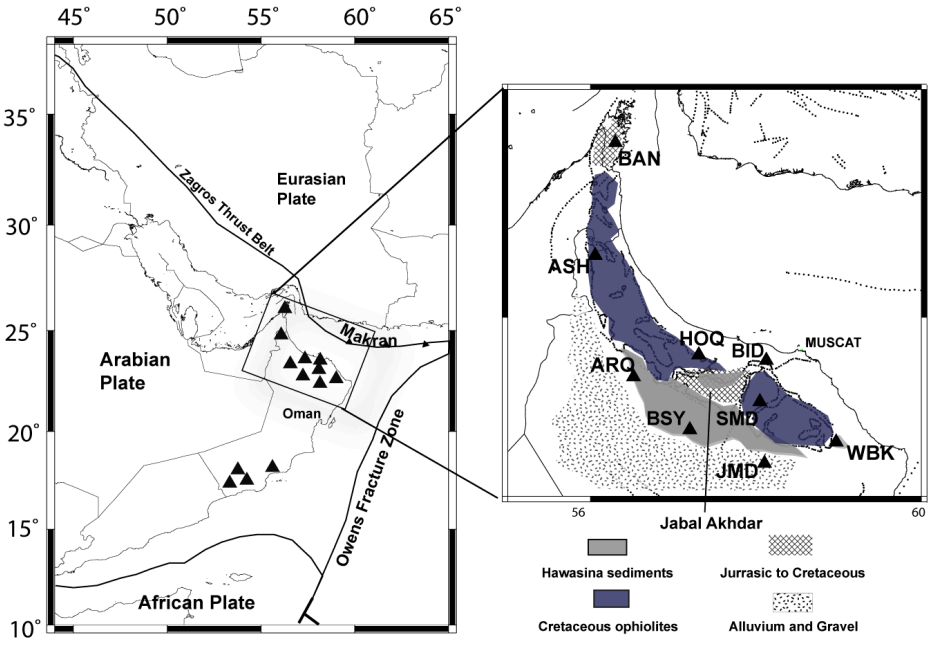

Figure 1

Tectonic setting of Northern Oman

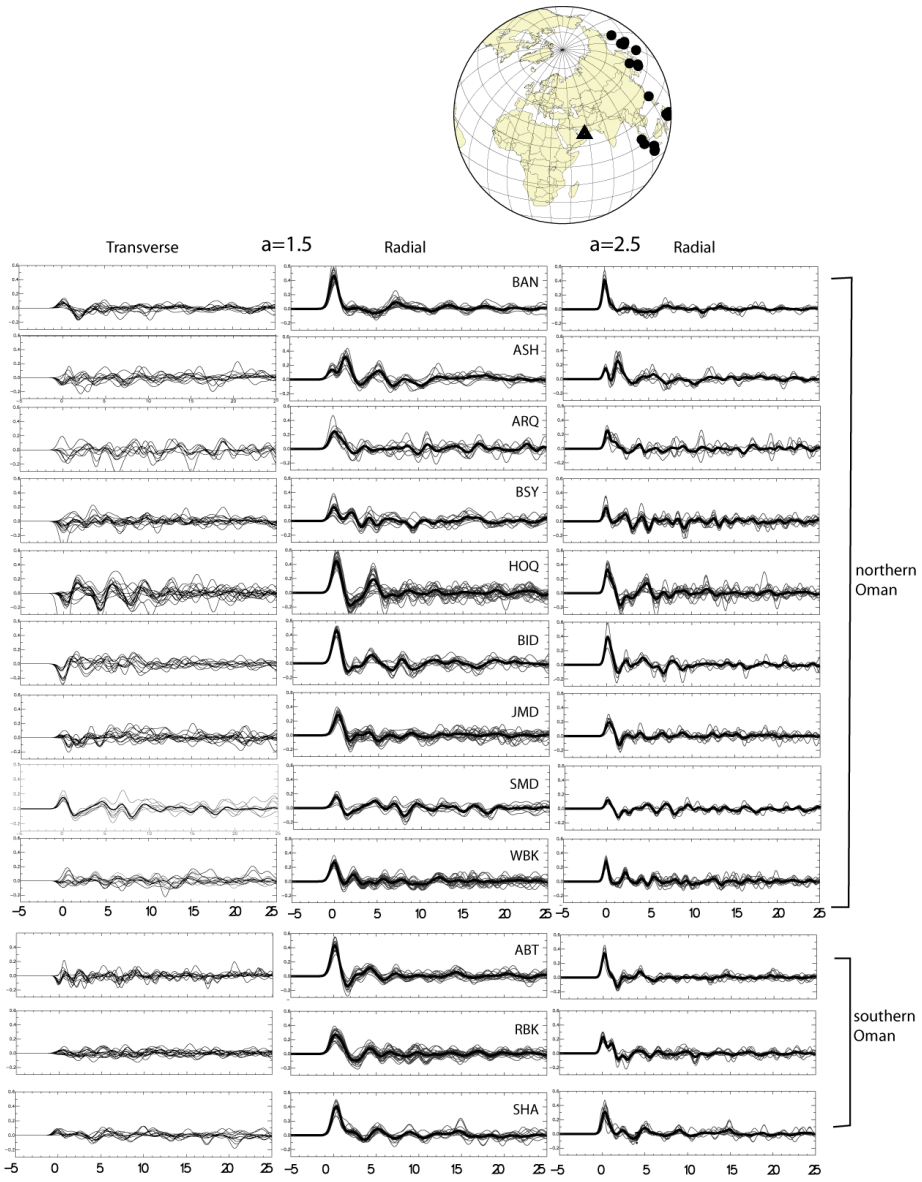

Figure 2

Receiver functions with low and high Gaussian filters respectively. SHA, ASH and BAN are broadband stations.

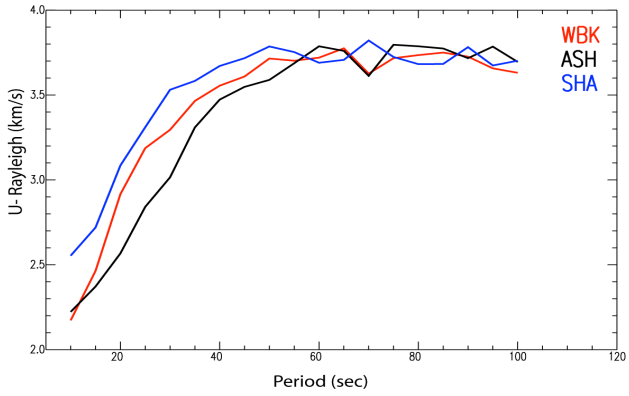

Figure 3

Dispersion curve plots of Rayleigh wave group velocities (Pasyanos, 2005). The blue (SHA) is located at Dhofar, red is east (WBK) and black (ASH) is the western part of Oman mountains. ASH is the slowest up to 50 sec

Table 1 Station location information together with Moho depths and Vp/Vs ratios at each station

STA	LAT	LON	Moho	Vp/Vs
ABT	**17.35**	**53.29**	**35**	**1.77±0.02**
ARQ	**23.34**	**56.52**	**40**	**1.60±0.10**
ASH	**24.68**	**56.06**	**45**	**1.79±0.03**
BAN	**25.92**	**56.3**	**48**	**1.93±0.02**
BID	**23.52**	**58.13**	**44**	**1.53±0.02**
BSY	**22.74**	**57.2**	**38**	**1.67±0.19**
HOQ	**23.58**	**57.31**	**40**	**1.76±0.10**
JMD	**22.37**	**58.1**	**43**	**1.53±0.03**
RBK	**17.5**	**54.2**	**34**	**1.81±0.01**
SHA	**18.02**	**55.62**	**34**	**2.00±0.01**
SMD	**23.06**	**58.05**	**38**	**1.71±0.03**
WBK	**22.61**	**58.97**	**46**	**1.73±0.05**
WHF	**17.92**	**53.77**	**36**	**1.79**

Figure 4 a. The inversion results for some of the stations. The black line is the data and reds are synthetic. Two starting models along with various influence parameters (p=0.3,0.5 and 0.7) and smoothness (0.6 and 0.7) used to obtain the final output. The sensitivity of the inversion is mostly observed at noisier stations e.g. BSY and HOQ. (*) indicates broad-band stations.

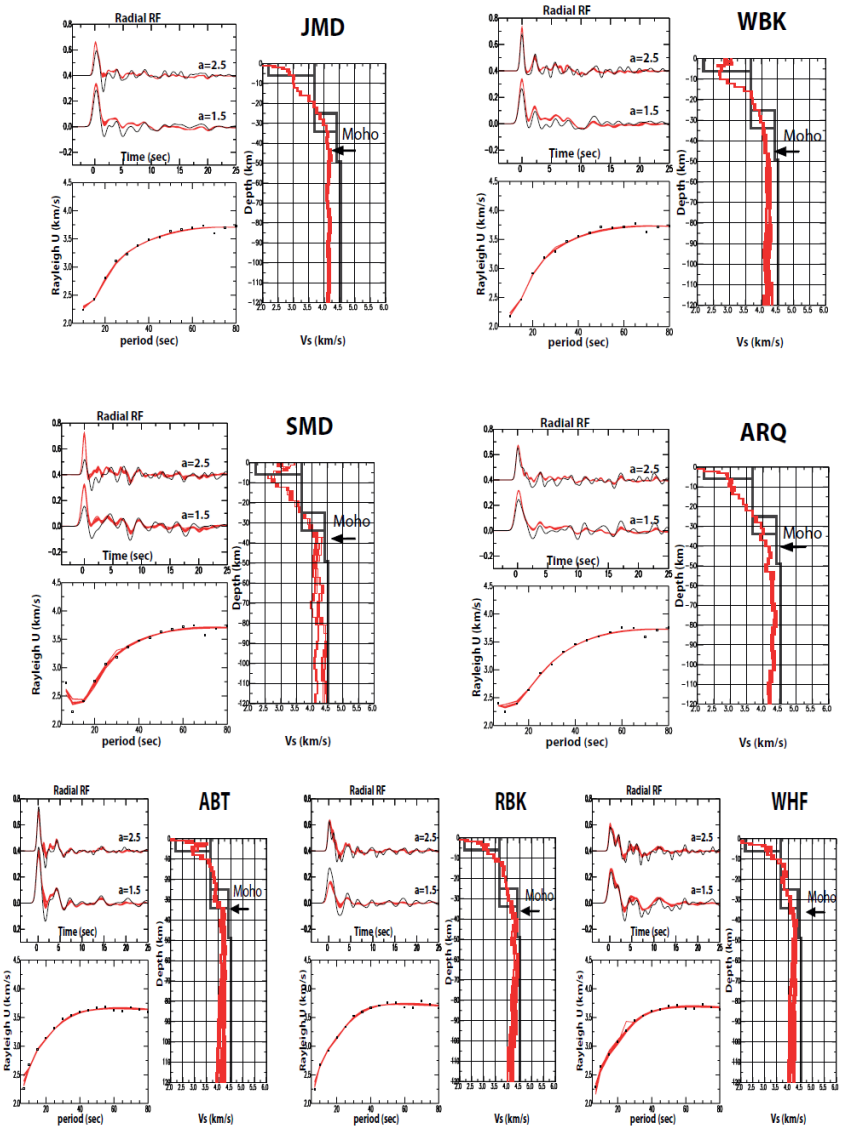

Figure 4 b. The inversion results for some of the stations. The black line is the data and reds are synthetic. Two starting models along with various influence parameters (p=0.3,0.5 and 0.7) and smoothness (0.6 and 0.7) used to obtain the final output.

salam95 3/27/11 12:32 PM
Formatted: Centered

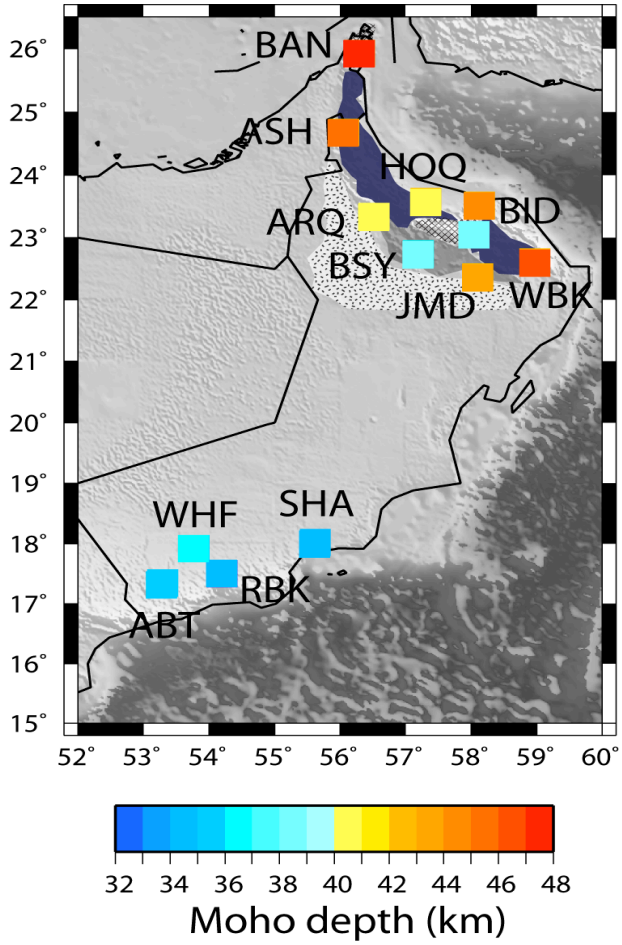

Figure 5

Moho depths color coded at each station. Note the thinner crust in Dhofar region. The thickest is observed at BAN and WBK.

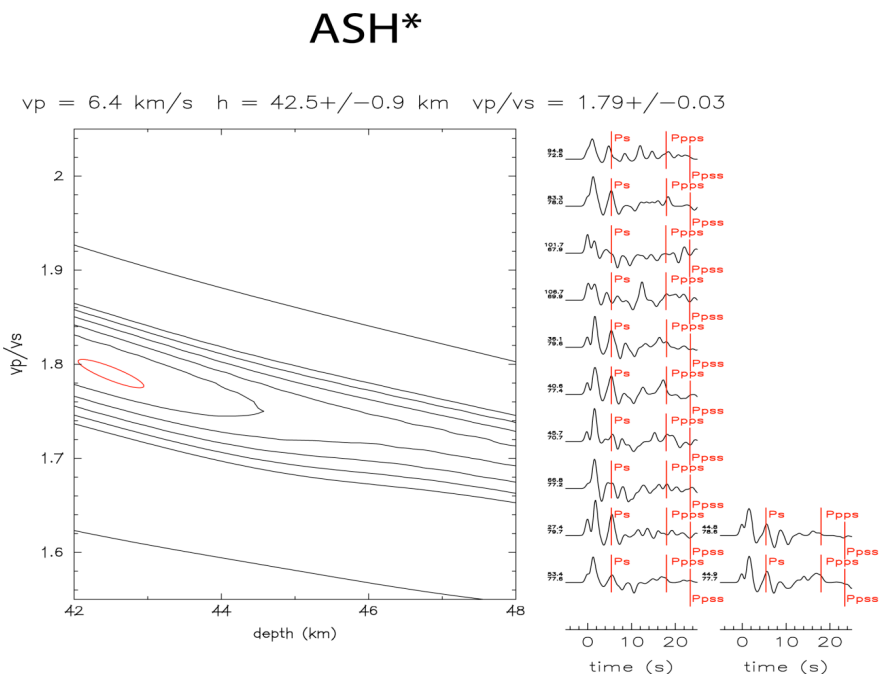

Figure 6. The amplitudes of grid-search stacking method are given in amplitudes and the theoretical onset times of maximum amplitudes on the waveforms.

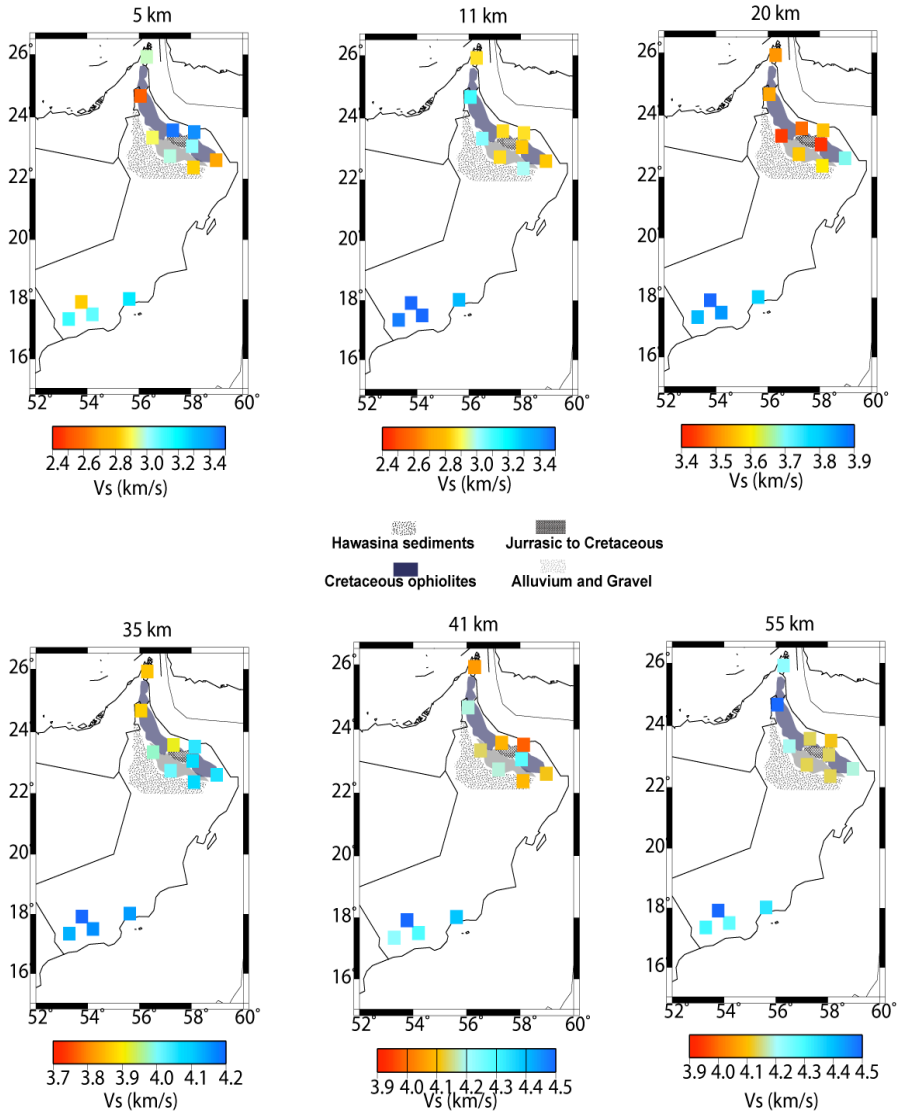

Figure 7

The shear wave velocities at various depths to present upper and lower crust, upper mantle velocities. The geologic units are shown with various patterns on each map.

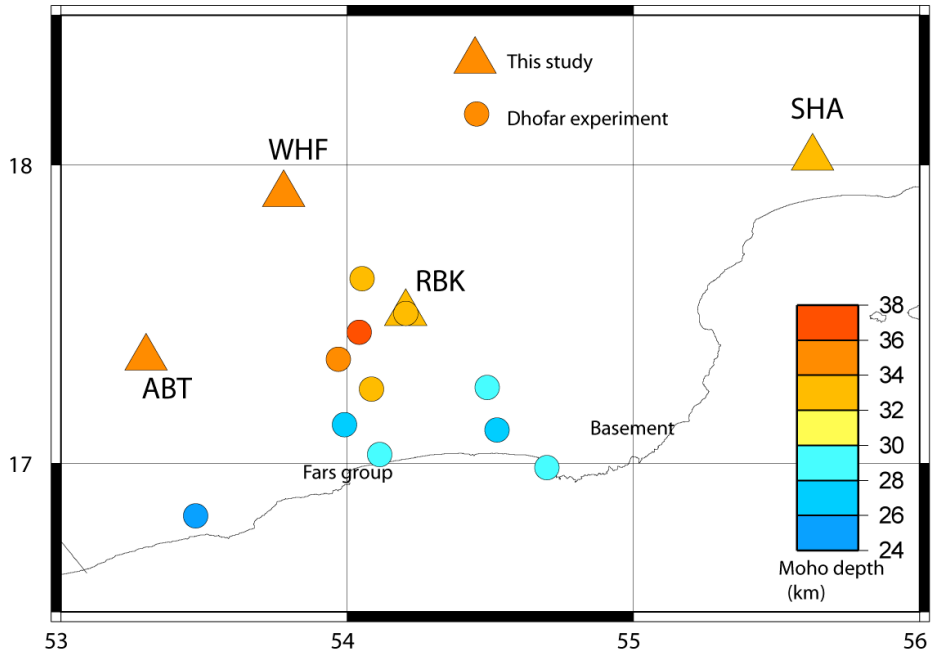

Figure 8 Triangles are the crustal thicknesses of this study and the circles are from Tiberi et al., (2007).